



HAL
open science

In vivo and in silico evaluation of a new nitric oxide donor, S,S' -dinitrosobucillamine

Marie-Lynda Bouressam, Benjamin Meyer, Ariane Boudier, Igor Clarot, Pierre Leroy, Alessandro Genoni, Manuel Ruiz-Lopez, Philippe Giummelly, Patrick Liminana, Valérie Salgues, et al.

► To cite this version:

Marie-Lynda Bouressam, Benjamin Meyer, Ariane Boudier, Igor Clarot, Pierre Leroy, et al.. In vivo and in silico evaluation of a new nitric oxide donor, S,S' -dinitrosobucillamine. *Nitric Oxide: Biology and Chemistry*, 2017, 71, pp.32-43. 10.1016/j.niox.2017.10.004 . hal-01665352

HAL Id: hal-01665352

<https://hal.univ-lorraine.fr/hal-01665352v1>

Submitted on 15 Dec 2017

HAL is a multi-disciplinary open access archive for the deposit and dissemination of scientific research documents, whether they are published or not. The documents may come from teaching and research institutions in France or abroad, or from public or private research centers.

L'archive ouverte pluridisciplinaire **HAL**, est destinée au dépôt et à la diffusion de documents scientifiques de niveau recherche, publiés ou non, émanant des établissements d'enseignement et de recherche français ou étrangers, des laboratoires publics ou privés.

1 ***IN VIVO AND IN SILICO* EVALUATION OF A NEW NITRIC OXIDE DONOR,**
2 ***S,S'*-DINITROSOBUCILLAMINE**

3
4
5 **Marie-Lynda BOURESSAM^a, Benjamin MEYER^{b,c}, Ariane BOUDIER^a, Igor**
6 **CLAROT^a, Pierre LEROY^a, Alessandro GENONI^{b,c}, Manuel RUIZ-LOPEZ^{b,c}, Philippe**
7 **GIUMMELLY^a, Patrick LIMINANA^a, Valérie SALGUES^a, Mostafa KOUACH^d,**
8 **Caroline PERRIN-SARRADO^a, Isabelle LARTAUD^a, François DUPUIS^a**

9
10 ^a Université de Lorraine, CITHEFOR EA 3452, Faculty of Pharmacy, BP 80403, F-54000
11 Nancy Cedex, France

12 ^b Université de Lorraine, SRSMC UMR 7565, Faculty of Sciences and Technologies, F-54500
13 Vandoeuvre-lès-Nancy, France

14 ^c CNRS, SRSMC UMR 7565, Faculty of Sciences and Technologies, F-54500 Vandoeuvre-
15 lès-Nancy, France

16 ^d Université de Lille 2, Plateau de Spectrométrie de Masse - GRITA EA 7365, Faculty of
17 Pharmacy, BP 83, F-59006 Lille, France

18 **CORRESPONDING AUTHOR** : François DUPUIS

19 CITHEFOR EA3452, Faculty of Pharmacy, 5 rue Albert Lebrun, BP 80403, F-54000 Nancy
20 Cedex, France

21 e-mail: Francois.Dupuis@univ-lorraine.fr

22 phone: +33 3 72 74 72 72

ABBREVIATIONS

BUC(NO)₂: *S,S'*-dinitrosobucillamine

BUC(SH)₂: bucillamine

GSNO: *S*-nitrosoglutathione

ISDN: isosorbide dinitrate

MAP: mean arterial pressure

NACNO: *S*-nitroso-*N*-acetylcysteine

PAP: pulse arterial pressure

RSNO(s): *S*-nitrosothiol(s)

SNAP: *S*-nitroso-*N*-acetylpenicillamine

SNOPCs: *S*-nitrosophytochelatin

SNP: sodium nitroprusside

23 **ABSTRACT**

24 **Purpose.** In a previous work, we have synthesized a new dinitrosothiol, *i.e.* *S,S'*-
25 dinitrosobucillamine BUC(NO)₂ combining *S*-nitroso-*N*-acetylpenicillamine (SNAP) and *S*-
26 nitroso-*N*-acetylcysteine (NACNO) in its structure. When exposed to isolated aorta, we
27 observed a 1.5-fold increase of [•]NO content and a more potent vasorelaxation (1 log higher
28 pD₂) compared to NACNO and SNAP alone or combined (Dahboul *et al.*, 2014). In the
29 present study, we analyzed the thermodynamics and kinetics for the release of [•]NO through
30 computational modeling techniques and correlated it to plasma assays. Then BUC(NO)₂ was
31 administered *in vivo* to rats, assuming it will induce higher and/or longer hypotensive effects
32 than its two constitutive *S*-mononitrosothiols.

33 **Methods.** Free energies for the release of [•]NO entities have been computed at the density
34 functional theory level assuming an implicit model for the aqueous environment. Degradation
35 products of BUC(NO)₂ were evaluated *in vitro* under heating and oxidizing conditions using
36 HPLC coupled with tandem mass spectrometry (MS/MS). Plasma from rats were spiked with
37 RSNO and kinetics of RSNO degradation was measured using the classical Griess-Saville
38 method. Blood pressure was measured in awake male Wistar rats using telemetry (n = 5, each
39 as its own control, 48 h wash-out periods between subcutaneous injections under transient
40 isoflurane anesthesia, random order: 7 mL/kg vehicle, 3.5, 7, 14 μmol/kg SNAP, NACNO,
41 BUC(NO)₂ and an equimolar mixture of SNAP+NACNO in order to mimic the number of
42 [•]NO contained in BUC(NO)₂). Variations of mean (ΔMAP, reflecting arterial dilation) and
43 pulse arterial pressures (ΔPAP, indirectly reflecting venodilation, used to determine effect
44 duration) *vs.* baseline were recorded for 4 h.

45 **Results.** Computational modeling highlights the fact that the release of the first [•]NO radical in
46 BUC(NO)₂ requires a free energy which is intermediate between the values obtained for
47 SNAP and NACNO. However, the release of the second [•]NO radical is significantly favored
48 by the concerted formation of an intramolecular disulfide bond. The corresponding oxidized
49 compound was also characterized as related substance obtained under degradation conditions.
50 The *in vitro* degradation rate of BUC(NO)₂ was significantly greater than for the other RSNO.
51 For equivalent low and medium [•]NO-load, BUC(NO)₂ produced a hypotension identical to
52 NACNO, SNAP and the equimolar mixture of SNAP+NACNO, but its effect was greater at
53 higher doses (-62±8 and -47±14 mmHg, maximum ΔMAP for BUC(NO)₂ and
54 SNAP+NACNO, respectively). Its duration of effect on PAP (-50%) lasted from 35 to 95 min,
55 *i.e.* shorter than for the other RSNO (from 90 to 135 min for the mixture SNAP+NACNO).

56 **Conclusion.** A faster metabolism explains the abilities of BUC(NO)₂ to release higher
57 amounts of [•]NO and to induce larger hypotension but shorter-lasting effects than those
58 induced by the SNAP + NACNO mixture, despite an equivalent [•]NO-load.

59 **Key-words**

60 *S,S'*-dinitrosobucillamine; telemetry; awake rat; mean arterial pressure; pulse arterial pressure;
61 *ab initio* calculations

1. INTRODUCTION

Decrease of nitric oxide ($\cdot\text{NO}$) bioavailability is associated with cardiovascular diseases such as hypertension, atherosclerosis, angina pectoris [1]. Currently available $\cdot\text{NO}$ donors induce tolerance and oxidative stress [2; 3]. *S*-nitrosothiols (RSNO) are interesting candidates for delivering $\cdot\text{NO}$ [4] as they do not induce such side effects [5]. They have a longer half-life [6], induce vasorelaxation [7], prevent platelet aggregation [8] and are currently thought to play a major role in the endogenous storage and transport of $\cdot\text{NO}$ [9; 10]. *S*-nitrosothiols have also the advantage of releasing both $\cdot\text{NO}$ and thiols which exhibit antioxidant and anti-inflammatory properties.

The rate and/or quantity of released $\cdot\text{NO}$ vary according to the thiol carrying the SNO moiety. Therefore, numerous molecules exhibiting thiol functions are under consideration to define the best RSNO candidate. An interesting strategy relies on increasing $\cdot\text{NO}$ -payload by synthesizing di- or poly-nitrosothiols. Such compounds may increase the amount of released $\cdot\text{NO}$, while limiting the drug quantity [11; 12] compared to most of the mononitrosothiols previously synthesized [9; 13]. Besides the $\cdot\text{NO}$ -payload, Heikal *et al.* evaluated the bioactivity of a new RSNO subgroup: *S*-nitrosophytochelatin (SNOPCs). These oligopeptides expressed in plants are analogues of *S*-nitrosoglutathione (GSNO, an endogenous RSNO present in humans). Heikal *et al.* compared several SNOPCs, carrying 2 to 6 SNO moieties, with GSNO. When administered at equal molar concentrations of SNO, SNOPCs induce a more intense decrease of blood pressure than GSNO [14], even though their *in vitro* vasodilatory effect was equivalent to GSNO (again at equimolar concentrations of SNO) [12]. These results demonstrate that the molecule carrying the SNO moieties is also a major determinant of the biological activities of RSNO.

We previously synthesized a new RSNO, *S,S'*-dinitrosobucillamine ($\text{BUC}(\text{NO})_2$), which combines in its structure two mononitrosothiols: *S*-nitroso-*N*-acetylpenicillamine (SNAP) and *S*-nitroso-*N*-acetylcysteine (NACNO) [11]. The synthesis was performed using bucillamine ($\text{BUC}(\text{SH})_2$) which is a commercially available drug used to treat rheumatoid arthritis, in relation with its anti-inflammatory and antioxidant properties [15; 16]. In an aortic ring model, $\text{BUC}(\text{NO})_2$ induced vasorelaxation at lower concentrations (pD_2 7.8 ± 0.1 , with $\text{pD}_2 = -\log \text{EC}_{50}$, *i.e.* the molar concentration producing 50% of the maximal effect) than NACNO (6.4 ± 0.2), SNAP (6.7 ± 0.1) and the mixture of SNAP+NACNO (6.7 ± 0.2). Furthermore, the *in vitro* $\cdot\text{NO}$ release was significantly higher from $\text{BUC}(\text{NO})_2$ (6-fold increase *versus* basal value) than from the SNAP+NACNO mixture (4-fold increase *versus* basal value) [11]. Altogether, these data suggest that $\text{BUC}(\text{NO})_2$ might be an interesting

96 candidate for the cardiovascular pathologies. However, those previous experiments did not
97 evaluate the systemic effects.

98 Therefore, the present work was conducted to further characterize BUC(NO)₂. In this
99 aim, we used molecular modeling to study the thermodynamics of the two [•]NO entities
100 released from BUC(NO)₂ and the resulting bucillamine derived product. We also monitored *in*
101 *vitro* the obtained degradation products by using HPLC-MS/MS, and examined *in vitro* in
102 plasma from Wistar rat spiked with RSNO the rate of decomposition of BUC(NO)₂ as
103 compared to SNAP, NACNO and SNAP+NACNO. Then, we explored the systemic effects
104 and duration of action of BUC(NO)₂ *in vivo*, using awake male Wistar rats equipped with
105 telemetric devices. On the basis of its [•]NO-release profile, we assume that BUC(NO)₂ would
106 induce higher and/or longer *in vivo* hypotensive effects than its constitutive *S*-mono-
107 nitrosothiols SNAP, NACNO. We also compare to an equimolar mixture of NACNO plus
108 SNAP (in order to mimic the quantity of [•]NO contained in the BUC(NO)₂ solutions). The
109 intensity of hypotension was evaluated on the basis of changes in mean arterial pressure
110 (MAP) which reflect the *in vivo* dilating effect of RSNO on arteries and arterioles. Changes in
111 pulse arterial pressure (PAP) were used to determine the duration of effect, as we previously
112 showed, using similar protocols, that PAP allows a precise evaluation of RSNO effects
113 duration [17; 18].

114 2. MATERIAL and METHODS

115 2.1. Reagents and standards

116 All reagents were of analytical grade and used without further purification. *N*-(2-
117 mercapto-2-methylpropanoyl)-*L*-cysteine (BUC(SH)₂) was purchased from Discovery Fine
118 Chemicals (Wimborne Dorset, United Kingdom). *N*-acetylpenicillamine (NAP), *N*-
119 acetylcysteine (NAC) and all other reagents were from Sigma-Aldrich (Saint Quentin
120 Fallavier, France). Ultrapure deionized water (> 18.2 MΩ.cm) was used to prepare all
121 solutions. Phosphate-buffered saline (PBS) was prepared as follows: [Na₂HPO₄] = 6.48 ×
122 10⁻³M, [KH₂PO₄] = 1.47 × 10⁻³M, [NaCl] = 137.93 × 10⁻³M, and [KCl] = 2.68 × 10⁻³M, final
123 pH was adjusted to 7.4 with NaOH (40%). All the RSNO were extemporaneously synthesized
124 at a final concentration of 10⁻² M, by reacting *N*-acetylpenicillamine, *N*-acetylcysteine or
125 BUC(SH)₂ with NaNO₂ in acidic medium, as previously described [11; 17; 19]. Solutions
126 were adjusted to pH 7.4 by adding NaOH 40% then two-fold diluted in 10⁻² M phosphate
127 buffer pH 7.4.

128 Final solutions showed high osmolarity (1.8 osm/L). The volumes and dilutions
129 required to reach isotonic solutions for injection were too important. Therefore, hyper-
130 osmolar solutions were used. Animals received the same volume for each injection (solutions
131 have been diluted according to the expected dose in a final volume of 3.4 mL). In the control
132 (vehicle) solution, nitrite ions were replaced by a 0.2 M NaCl solution.

133 Due to their light- and temperature-sensitivity, final solutions were stored in the dark
134 at 4°C, no longer than 5 days for NACNO and SNAP, and 10 h for BUC(NO)₂, according to
135 their stability previously described by Dahboul *et al.* [11].

136 **2.2. Theoretical chemistry calculations**

137 The computational approach was chosen according to our previous investigations [20].
138 Specifically, we performed Density Functional Theory calculations (B3PW91 functional [21]
139 with the 6-311+G(d,p) basis-set). In order to account for the influence of the physiological
140 medium, we assumed an ionized system (anionic form of the carboxylic group) surrounded by
141 an aqueous environment (described by an implicit solvation model [22]). A thorough analysis
142 of BUC(NO)₂ conformations was first performed. In the most stable structure, the peptide
143 bond is (as expected) in *trans* conformation and both RS-NO bonds adopt an *anti*
144 conformation. From this structure, we calculated the sequential homolytic bond dissociation
145 free energies (at 298.15 K) for the two RS-NO bonds. The two possible monoradical and the
146 biradical species were studied. Besides, we considered a hypothetical mechanism for the
147 second [•]NO dissociation in which the formation of an incipient disulfide bond significantly
148 stabilizes the process. All computations were carried out using the Gaussian09 package [23].

149 **2.3. Identification of degradation product(s) from S,S'-dinitrosobucillamine**

150 In order to check the reliability of the theoretical predictions, we have carried out LC-
151 MS/MS experiments aimed at identifying the molecular structure of a main degradation
152 product obtained after exposure of BUC(NO)₂ to either heating (55°C, 120 min) or H₂O₂
153 (10.0% v/v, 15 min). Such conditions have been previously used in the field of toxicology
154 predictions [24].

155 The stock BUC(NO)₂ solution (10⁻² M in phosphate buffer pH 7.4) with and without
156 H₂O₂ was diluted one thousand times in the mobile phase before injection in the LC system.

157 LC-MS/MS experiments were carried out on a UFLC-XR device (Shimadzu) coupled
158 to a QTRAP® 5500 MS/MS hybrid system triple quadrupole/linear ion trap mass
159 spectrometer (AB Sciex, Foster City, USA) equipped with a turbo VTM ion source.
160 Instrument control, data acquisition and processing were performed using Analyst 1.5.2
161 software. The RP-LC separation was carried out at 40°C on a Nucleosil C18 100 AB (5 μm

162 250 x 4 mm) column (Macherey Nagel) at a flow rate of 0.8 mL/min and with an isocratic
163 mobile phase CH₃CN-H₂O-HCOOH (30/69.9/0.1, v/v/v). The injection volume was 10 µL.
164 MS analysis was carried out in negative ionization mode using an ion spray voltage of -
165 4500V. The curtain gas flow was set at 25 psi using nitrogen. The turbo VTM ion source was
166 set at 550°C. Nebulizer gas and auxiliary gas flow (air) were set at 50 psi. Acquisition was
167 performed in IDA “Information Dependent Acquisition” method. The IDA method consists of
168 a switch between MS (survey scan) and MS/MS (dependent scan) in a single run.

169 **2.4. *In vitro* measurement of S,S'-dinitrosobucillamine degradation in spiked plasma**

170 In order to confirm our *in silico* and *in vitro* findings, we compared the rate of
171 degradation of BUC(NO)₂ *in vitro* to those of SNAP, NACNO and SNAP+NACNO. Briefly,
172 rats were anesthetized with isoflurane, heparinized (500 UI) and blood was collected on
173 heparinized tubes directly from the abdominal aorta. Blood was then centrifuged (2000g, 15
174 min, 4°C), plasma collected and immediately spiked with either BUC(NO)₂, SNAP, NACNO
175 or SNAP+NACNO (RSNO/plasma volume ratio of 1/10). Plasma samples were then stored
176 under agitation at 37°C.

177 The loading doses were chosen to achieve a plasma concentration of 175.0 µmol/L for
178 SNAP and NACNO and 87.5 µmol/L for SNAP+NACNO and BUC(NO)₂ (*i.e.* an equivalent
179 *NO-load of 175.0 µmol/L). These concentrations are equivalent to the theoretical maximal
180 concentrations following *in vivo* administration (7.0 µmol/kg for SNAP and NACNO and 3.5
181 µmol/kg for SNAP+NACNO and BUC(NO)₂, considering a total blood volume of 40 mL/kg).

182 The RSNO were quantified at 0, 5 and 15 min after RSNO load (based on the kinetics
183 of the *in vivo* blood pressure effect) by the Griess-Saville assay [25]. Briefly, the samples
184 were diluted in 0.4 M acetoacetic buffer (pH = 2.5) in duplicates (two dilutions tested, 1/20
185 and 1/50, final volume of 200 µL) and then incubated with 40 µL of a 0.6% (w/v)
186 sulfanilamide solution supplemented with 0.2% (w/v) of HgCl₂. The diazonium salt so formed
187 was reacted with 10 µL of a 0.6% (w/v) *N*-(1-naphthyl) ethylenediamine solution to form a
188 chromophoric azo product that absorbs at 540 nm. For each drug, the calibration curve was
189 made with the corresponding RSNO in phosphate buffer. Free nitrite ions (quantified by
190 Griess assay) as well as RSNO in non-fortified plasma were below the limit of detection (< 1
191 µmol/L) and could thus be neglected as regards to the RSNO load. Results are presented as a
192 percentage of the initial quantity of RSNO added to the plasma.

193 **2.5. Animals, telemetry and hemodynamics measurement**

194 All experiments were performed in accordance with the European Community
195 guidelines (2010/63/EU) for the use of experimental animals. The protocols and procedures

196 were approved by an advisory regional ethical committee on animal experiments (project
197 “BucNOtelem”, APAFIS#2119-2015100214406732 v3).

198 Surgery was performed on 4 month-old male normotensive outbred Wistar rats
199 (Rj/Han: Wi, Janvier, France) (n = 5) and the experiments conducted between 5 and 10
200 months of age. Animals had mild restriction to standard rat chow (A04, Safe, France, 25 g per
201 day) in order to maintain their body weight around 500 g until the end of experiments. They
202 drank water (Aqua-clear®, Culligan, USA) *ad libitum*. Rats were equipped with telemetric
203 devices (PA-C40, Data Sciences International, USA; abdominal aorta) under isoflurane
204 anesthesia and aseptic surgery (48 h analgesia with paracetamol 60 mg/kg/day *per os*, then 1
205 month recovery). Each rat was used as its own control. All the injections were performed
206 between 11 and 12 a.m., subcutaneously (21-G needle) under transient (less than 5 min)
207 isoflurane anesthesia in order to standardize injections [18] and to reduce stress. Each rat
208 received control solution, then, in a random order with 2-day wash-out period and at distinct
209 injection sites, SNAP, NACNO, BUC(NO)₂ or the mixture SNAP+NACNO at 3.5, 7, and 14
210 μmol/kg. At the end of the experiments, the effects of the RSNO were compared to that other
211 of •NO-donors, *i.e.* isosorbide dinitrate (ISDN, 21, 42 and 85 μmol/kg) and sodium
212 nitroprusside (SNP, from 0.0035 up to 3.5 μmol/kg). Animals were then euthanized
213 (pentobarbitone 120 mg/kg).

214 Hemodynamics were recorded in awake rats (Ponemah 5.1 software, Data Sciences
215 International, USA, 250 Hz sampling rate). Basal MAP (area under the pressure wave for
216 each valid cardiac cycle), PAP (difference between the maximum and minimum pressure
217 values of each pressure wave) and heart rate (HR) were recorded during minimum 2 h and
218 averaged on the last 5 min to obtain baseline values. For each RSNO dose, MAP, PAP and
219 HR were recorded continuously for 4 h following injection and their variations *vs.* baseline
220 values were averaged on 1 min every 5 min.

221 As mentioned above, changes in MAP were analyzed as RSNO are known to induce
222 arterial and arteriolar dilatation. Changes in PAP were analyzed as RSNO are known to
223 induce large venodilation [26]; we previously published a similar approach in [17; 18]. As
224 PAP cannot physiologically fall under 15 mmHg, this parameter is more suitable to accurately
225 determine the effect duration.

226 **2.6. Statistical analysis**

227 Results are expressed as means ± S.E.M.

228 Significant differences in *in vitro* RSNO degradation were determined by a two-way
229 ANOVA (variables: “time” and “drug”) followed by a *post-hoc* Bonferroni test.

230 Significant differences in MAP, PAP and HR variations between controls, SNAP,
231 NACNO, SNAP+NACNO or BUC(NO)₂ were determined at equivalent [•]NO-load (half dose
232 for SNAP+NACNO and BUC(NO)₂ *versus* mononitrosothiols) by a two-way ANOVA
233 (variables: “time” and “drug”) for repeated measurements (time factor) followed by a *post-*
234 *hoc* Bonferroni test.

235 The duration of effects on PAP, MAP and HR variations was evaluated individually as
236 the time of the last value remaining significantly lower (PAP and MAP) or higher (HR) than
237 the mean of the next 20 points. These durations and the maximal hypotension values were
238 then compared between groups by a two-way ANOVA (variables “dose” and “drug”)
239 followed by a *post-hoc* Bonferroni test.

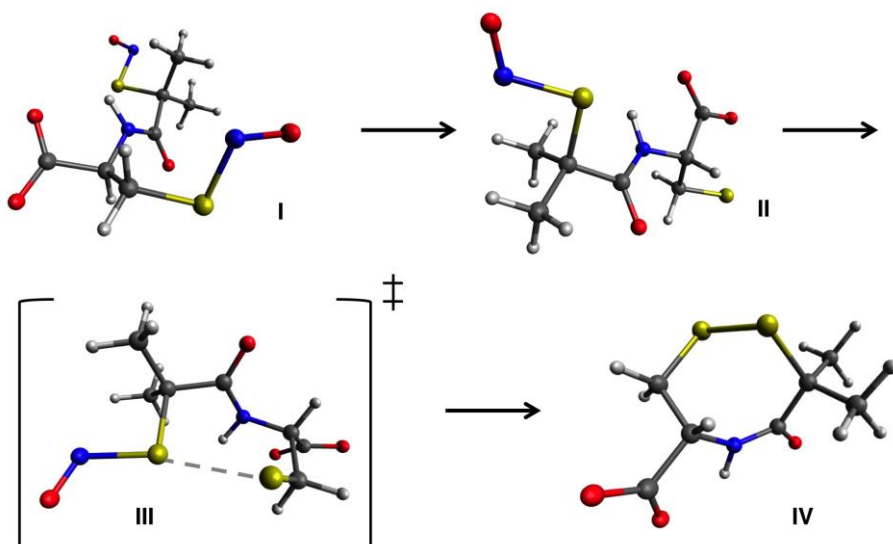
240 The null hypothesis was rejected at $p < 0.05$. Statistical analyzes were performed using
241 GraphPad Prism version 5 (GraphPad Software).

242 3. RESULTS

243 3.1. Thermodynamics of [•]NO release from *S,S'*-dinitrosobucillamine: computational 244 study

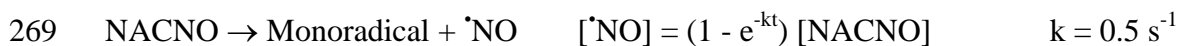
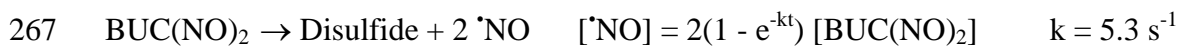
245 Since there are two different SNO groups in BUC(NO)₂, one can imagine two different
246 pathways, depending on which S-NO bond dissociates first. In the first pathway (P₁), the
247 primary SNO (*i.e.* the one attached to the RCH₂ group) dissociates first, and the sequential
248 [•]NO dissociation free energies, which are necessary to form the monoradical and the diradical
249 species, amount 16.4 and 16.9 kcal.mol⁻¹, respectively. In the second pathway (P₂), the tertiary
250 SNO (*i.e.* the one attached to the RC(CH₃)₂ group) dissociates first, and the corresponding
251 energies are 16.0 and 16.6 kcal.mol⁻¹.

252 The second dissociation process is much faster than the first one because of the
253 concerted formation of a disulfide bond, which substantially stabilizes the system.
254 Accordingly, the second dissociation proceeds through a transition structure that leads to a
255 disulfide product (Figure 1) and it is only 9.1 kcal.mol⁻¹ above the monoradical species in path
256 P₁ (or 12.3 kcal.mol⁻¹ in P₂). As a consequence of this low activation free energy for the
257 second dissociation process, in BUC(NO)₂ the first dissociation step can be considered the
258 rate determining for the double dissociation.



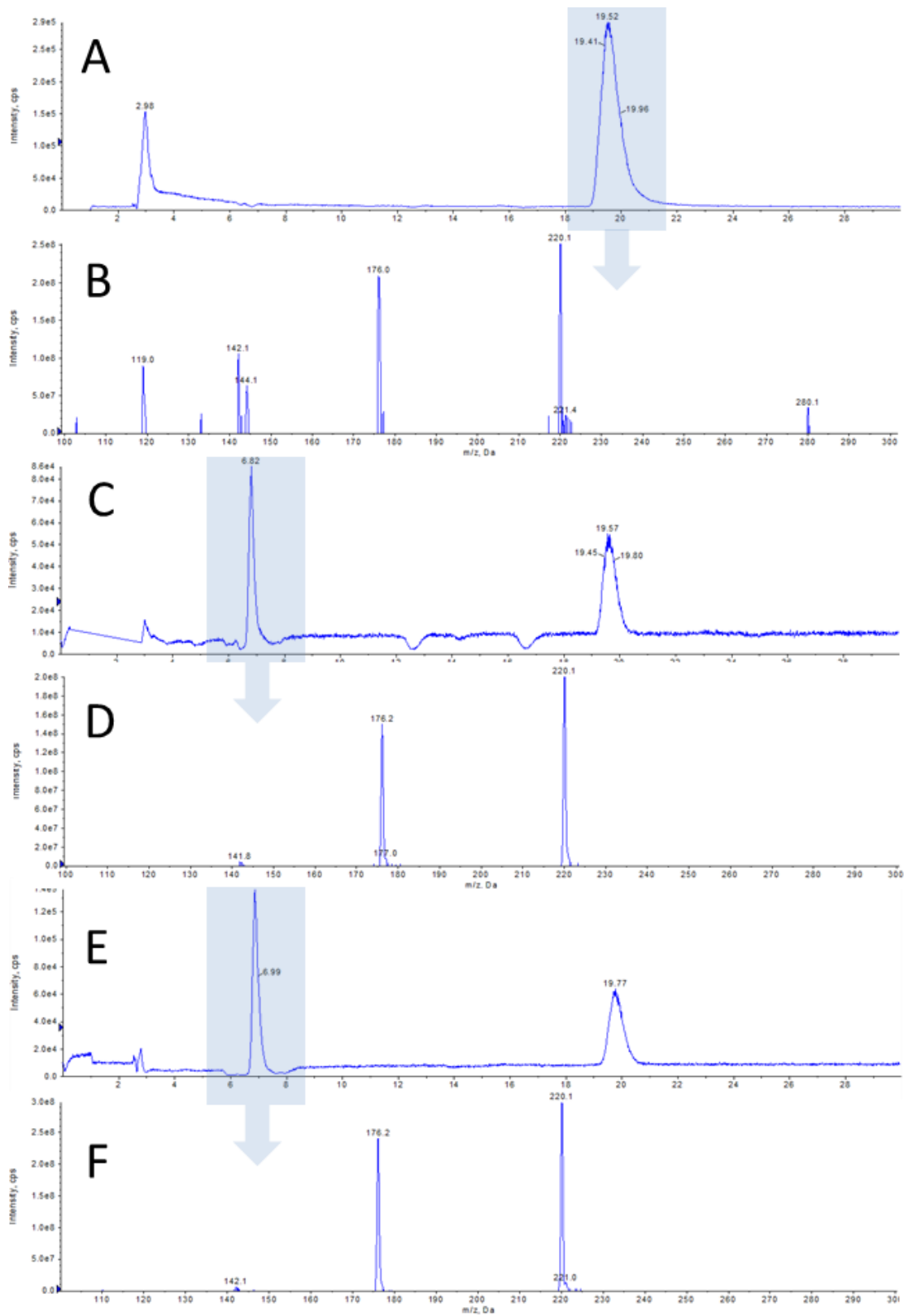
259
 260 **Figure 1. Calculated minimum energy structures for the double dissociation process of**
 261 **BUC(NO)₂ (I) along pathway P₁.**
 262 After the first (barrierless) [•]NO dissociation process leading to the monoradical (II), the
 263 system evolves through a transition structure (III) to form a disulfide-bond product (IV).

264 Applying transition state theory, and assuming first-order rate laws, the following
 265 kinetic constants have been roughly obtained from the quantum chemical models of
 266 BUC(NO)₂ (present work), SNAP and NACNO [20]:



270 3.2. Identification of the main degradation product of *S,S'*-dinitrosobucillamine

271 The degradation processes, monitored by mass-coupled liquid chromatography, led to
 272 similar results for both stress conditions. A chromatogram of a fresh BUC(NO)₂ solution is
 273 illustrated on Figure 2A with its MS/MS spectrum in Figure 2B showing a specific molecular
 274 ion at *m/z* 280. All the molecular structures determined in this part are described in Table 1.



275
 276
 277
 278
 279

Figure 2. MS (survey scan) chromatograms and corresponding MS/MS spectra of the grey peak obtained for the degradation study.
 Panels A and B: fresh solution; panels C and D: after 15 min with H₂O₂; panels E and F: after 120 min at 55°C.

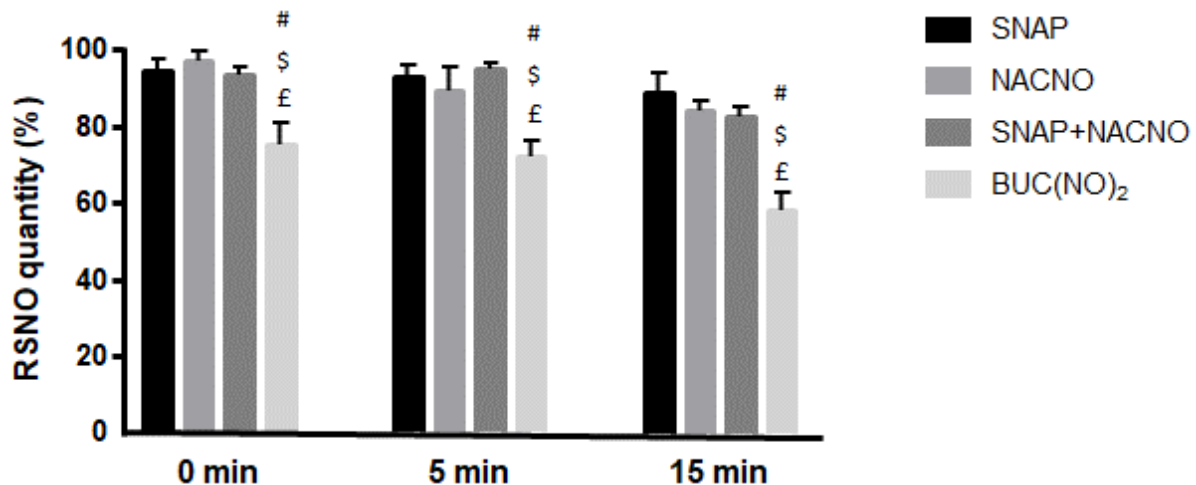
280 **Table 1: Mass/charge (m/z) values and structures of the molecular ions found in the**
281 **MS/MS spectra during the *in vitro* degradation study.**

m/z (amu)	Ions	Structures [X] ⁻
280	M ₁	BUC(S-NO,S-NO)-H
220	M ₂	BUC(S-S)-H
176	M ₃	M ₂ -CO ₂
144	M ₄	M ₃ -S
142	M ₅	M ₃ -SH ₂

282 Degradation conditions presently used led to the appearance of a chromatographic
283 peak at a retention time of 6.8 min. (Figure 2C and 2E for oxidation and heating,
284 respectively). The MS/MS spectra of this degradation product are given in Figure 2D and 2F
285 with a m/z major ion at 220 amu corresponding to the [BUC(S-S)-H]⁻ structure. It is important
286 to note that no other molecular ions were detected at m/z values upper than m/z 300, leading
287 to the conclusion that the disulfide bond formation is only favored through an intramolecular
288 pathway. Furthermore, the mononitrosated bucillamine was not observed whatever the
289 chromatogram under study, indicating that the denitrosation process is rapid and
290 simultaneously concerns the two thiol groups included in the BUC(NO)₂ structure.

291 **3.3.Kinetics for RSNO decomposition in plasma**

292 We added RSNO to plasma *in vitro*, to evaluate their decomposition rate. As shown in
293 Figure 3, a marked difference appears between BUC(NO)₂ and the other RSNO. At each time
294 point (0, 5 and 15 min), the *in vitro* degradation of BUC(NO)₂ was significantly greater than
295 that of SNAP, NACNO or SNAP+NACNO, indicating a faster metabolism and confirming
296 our *in silico* and *in vitro* findings.



297
 298 **Figure 3.** *In vitro* degradation rate of *S*-nitroso-*N*-acetylpenicillamine (SNAP), *S*-nitroso-*N*-acetylcysteine (NACNO), SNAP+NACNO and *S,S'*-dinitrosobucillamine (BUC(NO)₂).
 299 Each RSNO was added (to obtain a theoretical ^{*}NO concentration of 175 μmol/L) to freshly
 300 obtained plasma and quantified using the Griess-Saville assay (n= 9 to 14 per RSNO). Results
 301 are presented as percentage of the RSNO load (mean±SEM). $p_{\text{interaction}} = 0.0513$, p_{drug} and p_{time}
 302 $< 10^{-4}$; #: $p < 0,05$ vs SNAP; \$: $p < 0,05$ vs NACNO; £: $p < 0,05$ vs SNAP+NACNO (two-way
 303 ANOVA; *post-hoc* Bonferroni test).
 304

305 3.4. Haemodynamic responses to RSNO

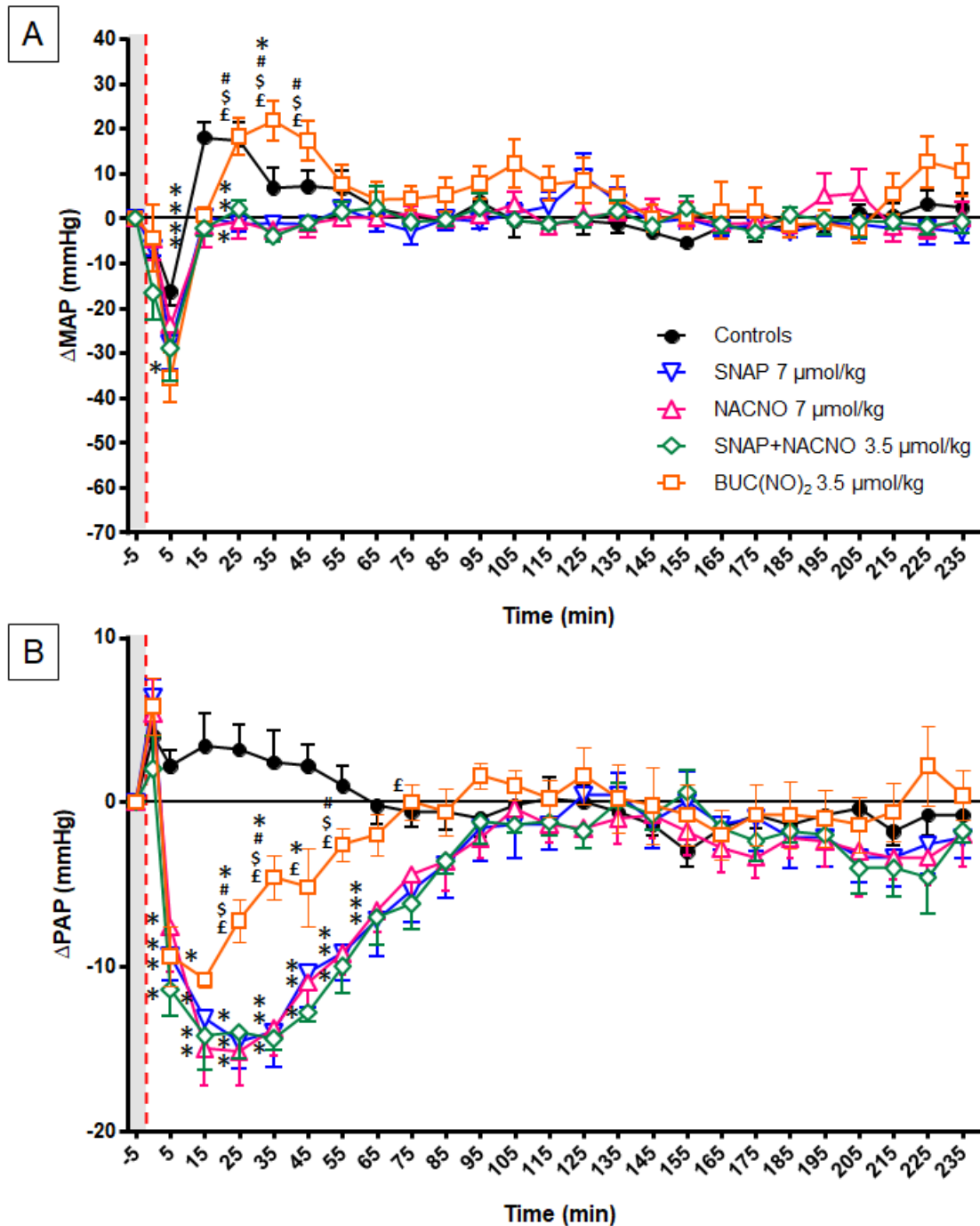
306 As previously observed when similar protocols are applied [17; 18], rats treated with
 307 the vehicle solution (controls) showed moderate increases in MAP (less than 20% vs.
 308 baseline, Figures 4 to 6) and HR (Figure 7) during the first 30 min after administration, related
 309 to the increase in activity during waking-up after the transient anesthesia. No significant
 310 change in PAP could be observed in controls (Figures 4 to 6).

311 The increases in MAP were masked when rats received RSNO, except for the lowest
 312 dose of BUC(NO)₂ (Figures 4 to 6). Each drug induced a dose-dependent hypotension (fall in
 313 MAP). When comparing the maximal hypotension produced by the different treatments, at
 314 doses that are expected to release similar amounts of ^{*}NO, there was no significant difference
 315 between BUC(NO)₂ and the SNAP+NACNO mixture at 3.5 and 7 μmol/kg, but a trend for a
 316 greater hypotension with BUC(NO)₂ compared to SNAP+NACNO at 14 μmol/kg (Table 2).
 317 The changes in MAP lasted from 5 (lowest doses) to 50 min (highest doses) with no
 318 significant differences amongst the treatments ($p_{\text{interaction}} = 0.0680$; $p_{\text{drug}} = 0.2418$; $p_{\text{dose}} < 10^{-4}$;
 319 data not shown).

320 These changes in MAP induced significant increases in HR (stimulation of the
 321 baroreflex) when compared to vehicle-treated animals (Figure 7). No noticeable difference

322 could be observed among the groups receiving RSNO. The duration of the changes in HR did
323 not differ amongst treatments, except for BUC(NO)₂ which induced a shorter effect than the
324 SNAP+NACNO mixture (Figure 8).

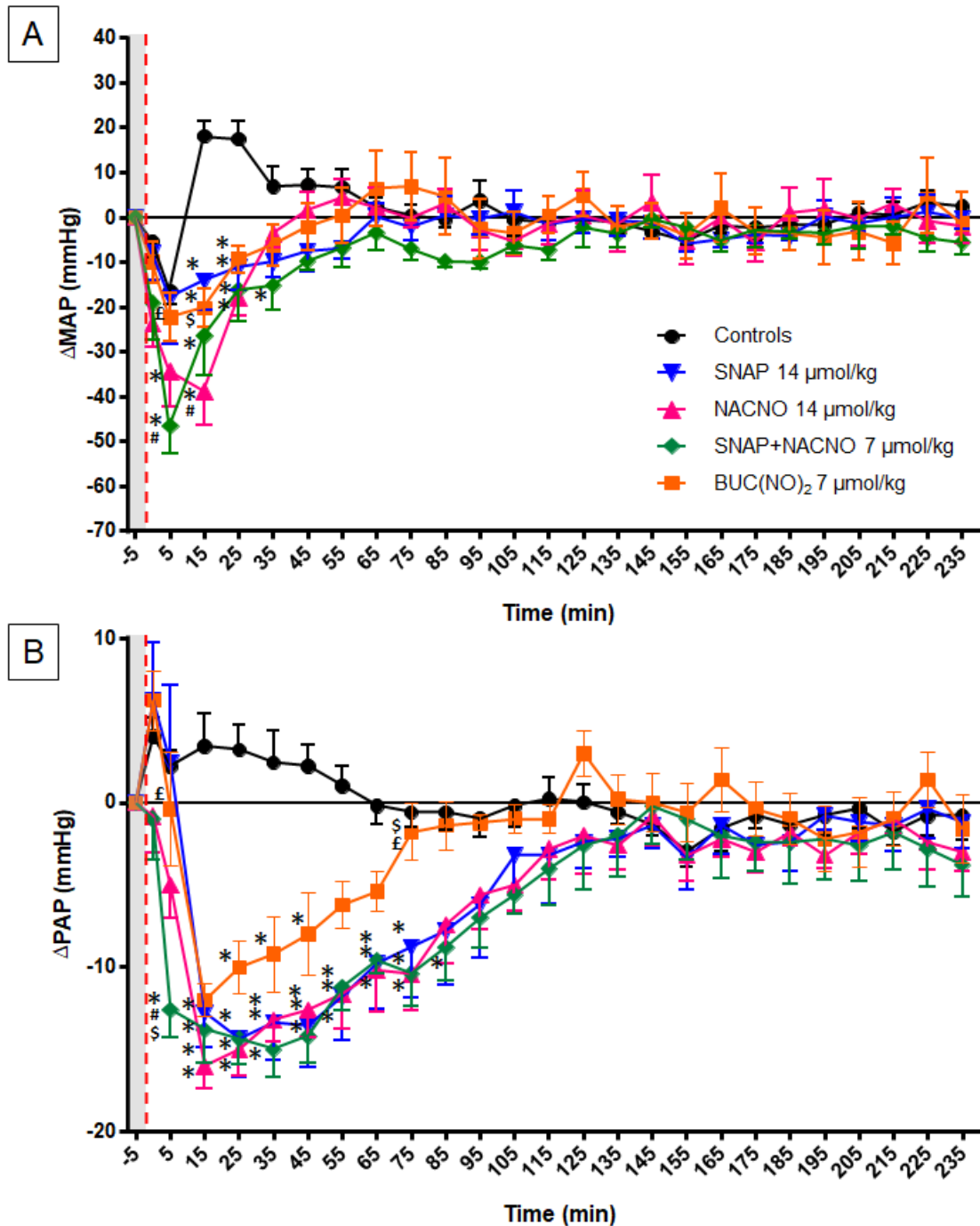
325 The duration of falls in PAP (around -15 mmHg for all drugs, whatever the doses used,
326 Figures 4 and 5) was dose-dependent. The effect of BUC(NO)₂ on PAP (from 37 to 96 min)
327 was significantly shorter than those of the other treatments (SNAP: 69 to 113 min; NACNO:
328 78 to 117 min) and the SNAP+NACNO mixture had the most prolonged impact on PAP (92
329 to 136 min, Figure 8).



330

331 **Figure 4. Impact of low doses of *S*-nitroso-*N*-acetylpenicillamine (SNAP), *S*-nitroso-*N*-**
 332 **acetylcysteine (NACNO), the mixture SNAP+NACNO and *S,S'*-dinitrosobucillamine**
 333 **(BUC(NO)₂) on mean arterial pressure (MAP, panel A) and pulse arterial pressure**
 334 **(PAP, panel B) variations (Δ) versus baseline.**

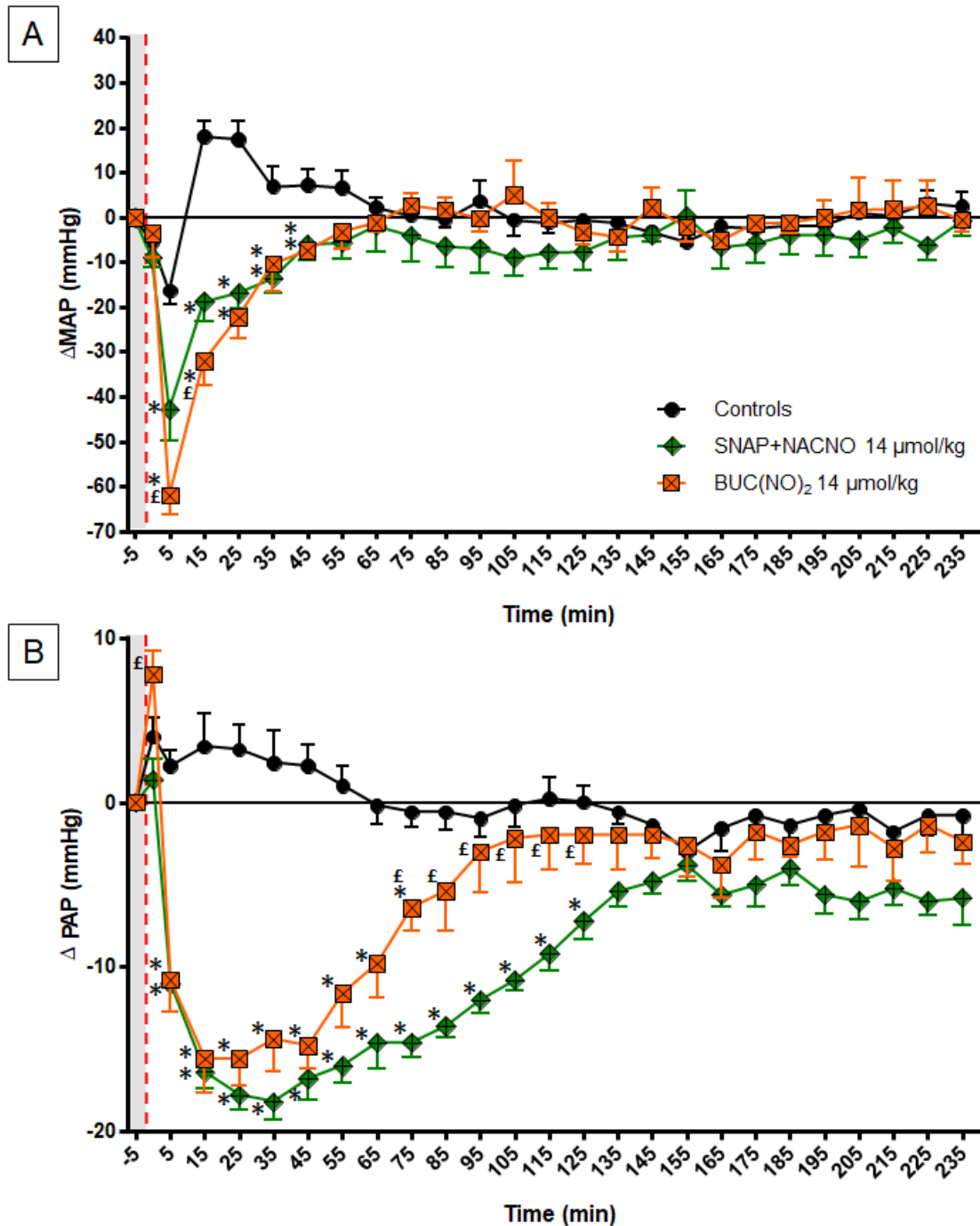
335 For a better clarity, only one out of two values was plotted on the graph. Doses were
 336 compared on the basis of an equivalent 'NO-load (half dose for SNAP+NACNO and
 337 BUC(NO)₂ versus mononitrosothiols). Each animal (n = 5) received all the drugs, each dose
 338 of each drug separated a by 2-day wash-out period. Grey boxes represent the duration of
 339 anesthesia and the red vertical dashed line the time of injection. *: p < 0,05 vs controls; #: p
 340 < 0,05 vs SNAP; \$: p < 0,05 vs NACNO; £: p < 0,05 vs SNAP+NACNO; Panel A: p_{interaction} <
 341 10⁻⁴; p_{drug} = 0.0688; p_{time} < 10⁻⁴; Panel B: p_{interaction} < 10⁻⁴; p_{drug} = 0.0210; p_{time} < 10⁻⁴; (two-
 342 way ANOVA; *post-hoc* Bonferroni test).



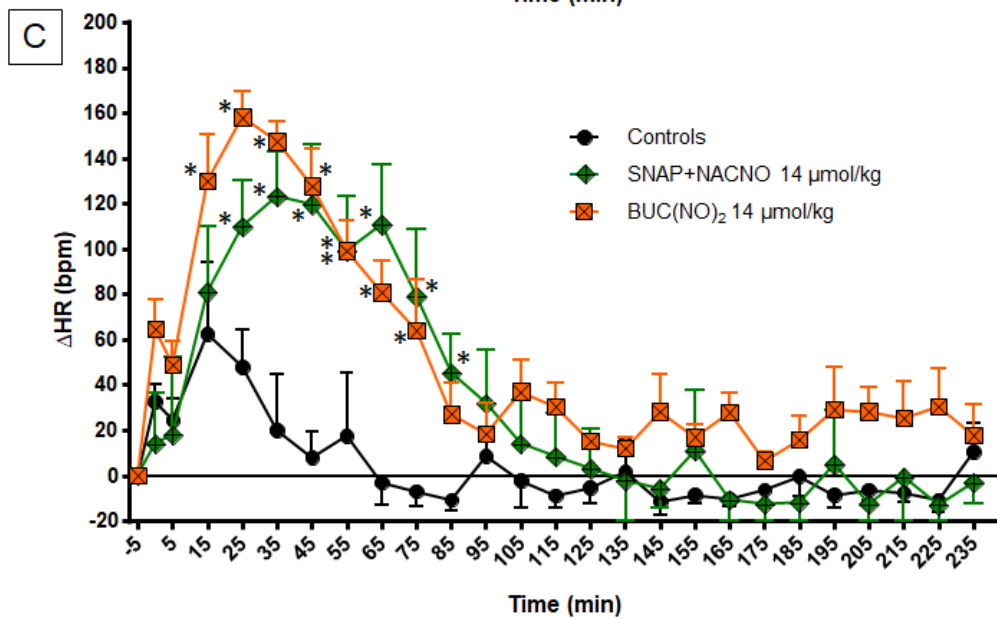
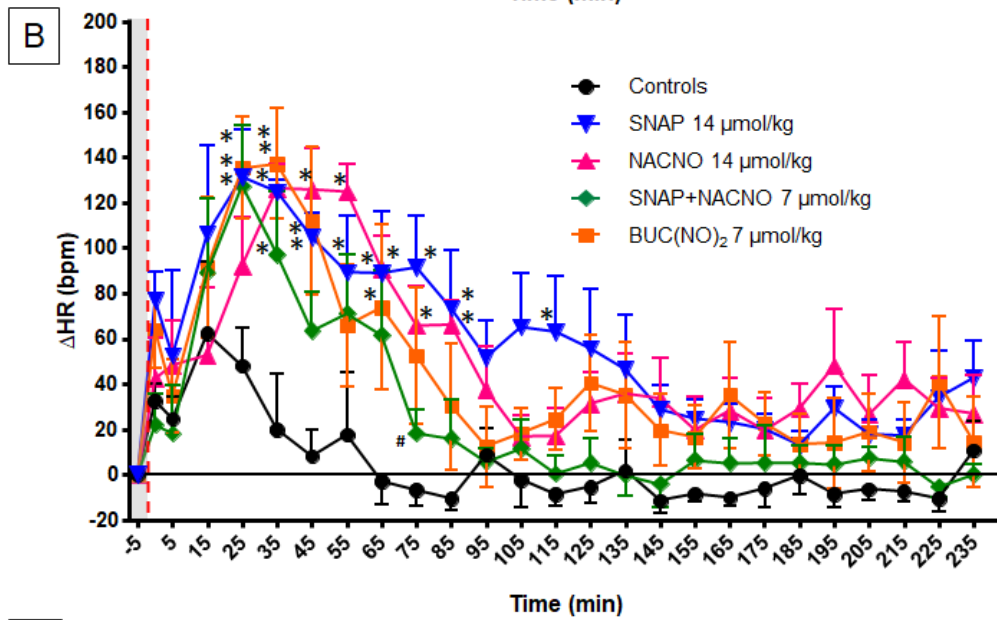
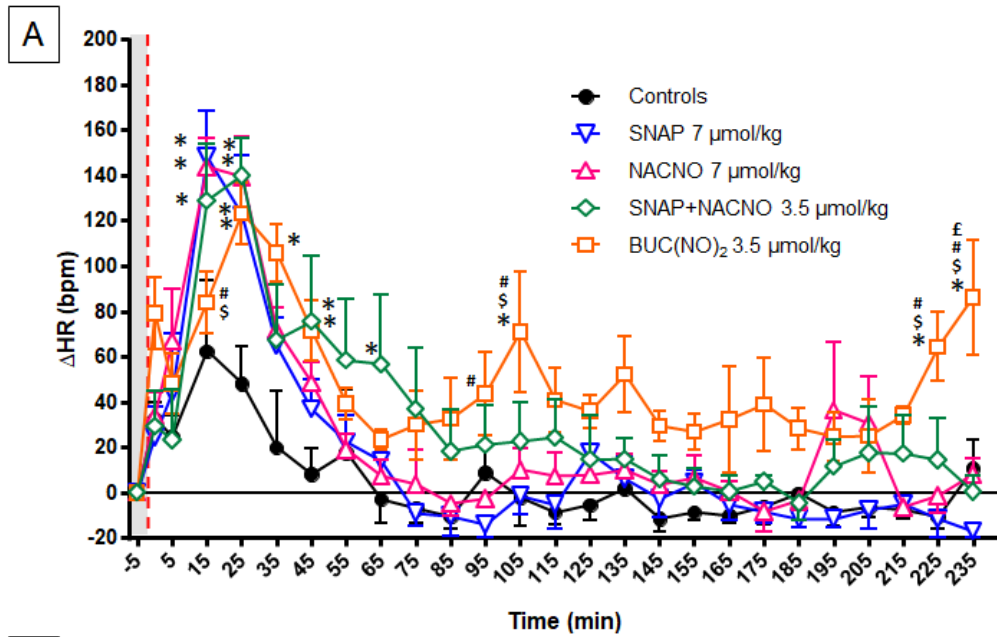
343

344 **Figure 5. Impact of medium doses of *S*-nitroso-*N*-acetylpenicillamine (SNAP), *S*-nitroso-**
 345 ***N*-acetylcysteine (NACNO), the mixture SNAP+NACNO and *S,S'*-dinitrosobucillamine**
 346 **(BUC(NO)₂) on mean arterial pressure (MAP, panel A) and pulse arterial pressure**
 347 **(PAP, panel B) variations (Δ) versus baseline.**

348 For a better clarity, only one out of two values was plotted on the graph. Doses were
 349 compared on the basis of an equivalent 'NO-load (half dose for SNAP+NACNO and
 350 BUC(NO)₂ versus mononitrosothiols). Each animal (n = 5) received all the drugs, each dose
 351 of each drug separated a by 2-day wash-out period. Grey boxes represent the duration of
 352 anesthesia and the red vertical dashed line the time of injection. *: p < 0,05 vs controls; #: p
 353 < 0,05 vs SNAP; \$: p < 0,05 vs NACNO; £: p < 0,05 vs SNAP+NACNO; Panel A: p_{interaction} <
 354 10⁻⁴; p_{drug} = 0.2498; p_{time} < 10⁻⁴; Panel B: p_{interaction} < 10⁻⁴; p_{drug} = 0.0421; p_{time} < 10⁻⁴; (two-
 355 way ANOVA; *post-hoc* Bonferroni test).



356
 357 **6. Impact of high doses of the mixture *S*-nitroso-*N*-acetylpenicillamine + *S*-nitroso-*N*-**
 358 **acetylcysteine (SNAP+NACNO) and *S,S'*-dinitrosobucillamine (BUC(NO)₂) on mean**
 359 **arterial pressure (MAP, panel A) and pulse arterial pressure (PAP, panel B) variations**
 360 **(Δ) versus baseline.**
 361 For a better clarity, only one out of two values was plotted on the graph. Each animal (n = 5)
 362 received all the drugs, each dose of each drug separated a by 2-day wash-out period. Grey
 363 boxes represent the duration of anesthesia and the red vertical dashed line the time of
 364 injection. *: p < 0,05 vs controls; £: p < 0,05 vs SNAP+NACNO; Panel A: p_{interaction} < 10⁻⁴; p_{drug}
 365 = 0.0979; p_{time} < 10⁻⁴; Panel B: p_{interaction} < 10⁻⁴; p_{drug} = 0.0003; p_{time} < 10⁻⁴; (two-way
 366 ANOVA; *post-hoc* Bonferroni test).



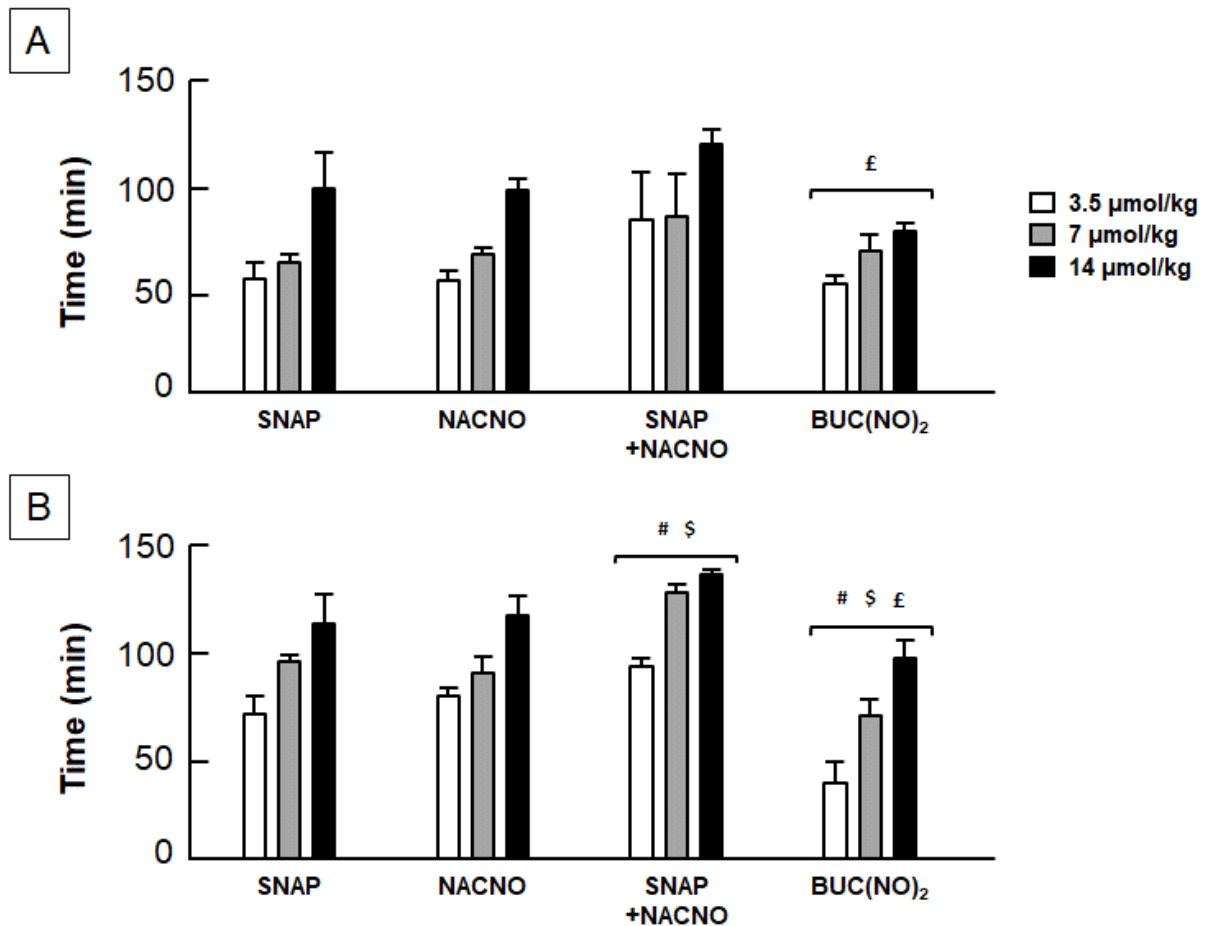
368 **Figure 7. Impact of low (panel A), medium (panel B) and high (panel C) doses of S-**
 369 **nitroso-N-acetylpenicillamine (SNAP), S-nitroso-N-acetylcysteine (NACNO), the**
 370 **mixture SNAP+NACNO and S,S'-dinitrosobucillamine (BUC(NO)₂) on heart rate**
 371 **variations (Δ HR) versus baseline.**

372 For a better clarity, only one out of two values was plotted on the graph. Doses were
 373 compared on the basis of an equivalent NO-load (half dose for SNAP+NACNO and
 374 BUC(NO)₂ versus mononitrosothiols). Each animal (n = 5) received all the drugs, each dose
 375 of each drug separated a by 2-day wash-out period. Grey boxes represent the duration of
 376 anesthesia and the red vertical dashed line the time of injection. *: p < 0,05 vs controls; #: p
 377 < 0,05 vs SNAP; \$: p < 0,05 vs NACNO; £: p < 0,05 vs SNAP+NACNO; Panel A: p_{interaction} <
 378 10⁻⁴; p_{drug} = 0.0007; p_{time} < 10⁻⁴; Panel B: p_{interaction} = 0.0853; p_{drug} = 0.0044; p_{time} < 10⁻⁴; Panel
 379 C: p_{interaction} < 10⁻⁴; p_{drug} = 0.0260; p_{time} < 10⁻⁴; (two-way ANOVA; *post-hoc* Bonferroni test).

380 **Table 2. Maximal mean arterial pressure effects of S-nitroso-N-acetylpenicillamine**
 381 **(SNAP), S-nitroso-N-acetylcysteine (NACNO), SNAP+NACNO and S,S'-**
 382 **dinitrosobucillamine (BUC(NO)₂).**

383 p_{interaction} = 0.1463, p_{dose} = 0.0009 and p_{drug} = 0.0090 (two-way ANOVA; *post-hoc* Bonferroni
 384 test).

Dose (μ mol/kg)	SNAP			NACNO			SNAP+NACNO			BUC(NO) ₂		
	3.5	7	14	3.5	7	14	3.5	7	14	3.5	7	14
Δ MAP (mmHg)	-18 \pm 6	-28 \pm 6	-28 \pm 10	-16 \pm 7	-24 \pm 11	-46 \pm 6	-29 \pm 2	-47 \pm 6	-43 \pm 7	-36 \pm 5	-29 \pm 5	-62 \pm 4



385
 386 **Figure 8. Duration of effect of *S*-nitroso-*N*-acetylpenicillamine (SNAP), *S*-nitroso-*N*-**
 387 **acetylcysteine (NACNO), the mixture SNAP + NACNO and *S,S'*-dinitrosobucillamine**
 388 **(BUC(NO)₂) on heart rate (HR, panel A) and pulse arterial pressure (PAP, Panel B).**
 389 #: $p < 0,05$ vs SNAP; \$: $p < 0,05$ vs NACNO; £: $p < 0,05$ vs SNAP+NACNO; Panel A: $p_{\text{interaction}}$
 390 = 0.6248; p_{drug} and $p_{\text{dose}} < 10^{-4}$; Panel B: $p_{\text{interaction}} = 0.9232$; $p_{\text{drug}} = 0.0127$; $p_{\text{dose}} < 10^{-4}$; (two-
 391 way ANOVA; *post-hoc* Bonferroni test).

392 **4. DISCUSSION**

393 *S,S'*-dinitrosobucillamine seems to induce large and fast release of [•]NO *in vivo*, as
 394 reflected by the stronger hypotension than the [•]NO-equimolar dose of SNAP+NACNO
 395 mixture (14 μmol/kg) and the shorter duration of effect on PAP compared to other RSNO.
 396 This parallels the *in vitro* results obtained in previous studies realized on isolated aortic rings,
 397 in which BUC(NO)₂ induced relaxation for the smallest concentration (Table 3, and [11]).

398 **Table 3. Physicochemical and *ex vivo* vasorelaxant properties of *S*-nitroso-*N*-**
 399 **acetylpenicillamine (SNAP), *S*-nitroso-*N*-acetylcysteine (NACNO), SNAP+NACNO and**
 400 ***S,S'*-dinitrosobucillamine (BUC(NO)₂).**

401 Stability (expressed as RSNO half-life) was determined in a Krebs medium at 37°C, pH 7.4.
 402 Hydrophobicity, determined by the partition coefficient (clog P), and [•]NO/RSNO mass ratio
 403 were calculated from ChemDraw software (CambridgeSoft, Perkin-Elmer, USA). The [•]NO
 404 content ([NO_x]) released from Wistar rat aortic rings exposed to RSNO was measured using
 405 the fluorogenic probe DAF-2 DA (4,5-diaminofluorescein diacetate). The vasorelaxant effects
 406 were evaluated *via* the pD₂ values (-log EC₅₀) from concentration response curves of isolated
 407 aortic rings precontracted with phenylephrine. Results are issued from [11].

	Half-life (h)	clog P	[•] NO/RSNO mass ratio	[NO _x] (μM)	pD ₂
SNAP	5	0.08	0.16	-	6.7
NACNO	63	- 0.46	0.14	-	6.4
SNAP+NACNO	-	-	0.15	420	6.7
BUC(NO) ₂	13	1.08	0.21	650	7.8

408 In the present study, changes in PAP were used to evaluate the duration of the RSNO effects.
 409 PAP is a function of arterial compliance/elastance, cardiac output and arterial tone, neither of
 410 which were measured in the present study as the protocols would have been too stressful for
 411 the animals. However, we used the duration of effect on PAP as a measure of the duration of
 412 the effect of RSNO, as (i) we previously published similar approach in [17; 18] and (ii) RSNO
 413 are known to induce large venodilation [26]. Venodilation decreases venous return and
 414 cardiac preload and thus decreases stroke volume, the main factor controlling PAP. Therefore,
 415 PAP would decrease. We previously showed by direct measurements of aortic pulse wave
 416 velocity [27] that [•]NO-donor administration did not change the second factor controlling PAP,
 417 *i.e.* aortic wall elasticity. We thus suggest that the fall in PAP is most likely related to a fall in
 418 stroke volume consecutive to venodilation. However, we cannot rule out that other factors are
 419 involved in the effect of RSNO on stroke volume and PAP. A direct positive myocardial
 420 effect of RSNO [28] and the improvement of cardiac function due to hypotension-induced
 421 decrease in cardiac afterload or to baroreflex-stimulated sympathetic response might both
 422 compensate the fall in stroke volume and reduce or shorten the impact of RSNO on PAP.

423 We did not correlate these durations with plasmatic levels of the drugs as
424 pharmacokinetics of RSNO and/or $\cdot\text{NO}$ remain difficult to perform *in vivo*. The literature
425 classically describes numerous pre-analytical and analytical difficulties to monitor plasma
426 concentrations of RSNO such as S-nitrosoglutathione (GSNO) [29], in relationship with their
427 poor stability (*e.g.* light, temperature and enzymes) [30]. For example, physiological
428 concentration of GSNO is still a matter of debate, ranging from 0.00135 ± 0.00046 to $1.78 \pm$
429 $0.76 \mu\text{M}$ [29]. In their recent paper [14], Heikal *et al.* attempted to evaluate the
430 pharmacokinetic profiles of GSNO and SNOPCs by measuring both the total RSNO content
431 in fractionated blood (plasma *vs.* blood cells) using gas-phase chemiluminescence reaction
432 with ozone and the total nitrate and nitrite species (NO_x) using a Griess colorimetric-based
433 method. Despite marked differences in hemodynamic effects, they failed to see any difference
434 in the pharmacokinetic profiles of these drugs, suggesting that blood monitoring of total
435 RSNO and NO_x might not be sensitive enough to enable the determination of the
436 pharmacokinetic profiles of RSNO.

437 In order to assess the metabolism of $\text{BUC}(\text{NO})_2$, we used an *in vitro* approach
438 consisting in loading freshly prepared plasma with RSNO. In this biological environment, we
439 observed a significant faster degradation of $\text{BUC}(\text{NO})_2$ compared with the other RSNO. Even
440 though this approach cannot be considered as a pharmacokinetic study, these results are
441 consistent with our *in silico* and *in vivo* results and seem to confirm a faster metabolism for
442 $\text{BUC}(\text{NO})_2$.

443 Assuming a 100% $\cdot\text{NO}$ release, we compared, with respect to the molar concentrations
444 of $\cdot\text{NO}$, the effects of the dinitrosothiol $\text{BUC}(\text{NO})_2$ and the SNAP+NACNO mixture,
445 mononitrosothiols and other $\cdot\text{NO}$ -donors, *i.e.* isosorbide dinitrate (ISDN) and sodium
446 nitroprusside (SNP) (Table 4). For a similar $\cdot\text{NO}$ -load, $\text{BUC}(\text{NO})_2$ induces the shortest effects.
447 The duration of its effects is half of the value obtained with SNAP+NACNO mixture and it is
448 no longer than that of mononitrosothiols such as GSNO (Table 4 and [17; 18]). When ISDN
449 was injected subcutaneously, it did not induce any significant hypotension but a 15 mmHg
450 decrease in PAP which lasted 37 min even at very high doses. Concerning SNP, the efficient
451 dose to induce hypotension was $0.35 \mu\text{mol/kg}$ (0.0035 and $0.035 \mu\text{mol/kg}$ had no effect), with
452 a -17 mmHg decrease in PAP lasting almost 100 min. At the dose of $3.5 \mu\text{mol/kg}$, 2 out of the
453 5 rats died while the remaining ones underwent severe and prolonged hypotension (which led
454 us to sacrifice the rats for exceeding the ethical limit points). These data led to several
455 assumptions.

456 **Table 4. Decreases in mean and pulse arterial pressures and duration of effects of S-**
 457 **nitroso-N-acetylpenicillamine (SNAP), S-nitroso-N-acetylcysteine (NACNO),**
 458 **SNAP+NACNO, S,S'-dinitrosobucillamine (BUC(NO)₂), S-nitrosogluthathione (GSNO),**
 459 **isosorbide dinitrate (ISDN) and sodium nitroprusside (SNP) at different doses and *NO -**
 460 **loads (subcutaneous administration).**

Molecule	Dose (μmol/kg)	*NO-load (μmol/kg)	ΔMAP (mmHg)	Duration PAP (min)	Reference
SNAP	7.0	7	-28	95	Present results
NACNO	7.0	7	-24	89	
SNAP+NACNO	3.5	7	-29	92	
BUC(NO) ₂	3.5	7	-36	37	
SNAP	17.0	17	-27	65	[17]
SNAP	14.0	14	-28	113	Present results
NACNO	14.0	14	-46	117	
SNAP+NACNO	7.0	14	-47	128	
BUC(NO) ₂	7.0	14	-29	69	
GSNO	11.0	11	-24	60	[18]
SNAP	34.0	34	-30	85	[17]
SNAP+NACNO	14.0	28	-43	136	Present results
BUC(NO) ₂	14.0	28	-62	96	
GSNO	22.0	22	-37	65	[18]
ISDN	21.0 (42.0, 85.0)	42 (84, 170)	No effect	37	Present results
SNP	0.035	0.035	No effect	No effect	
SNP	0.35	0.35	-49	96	

461 First, all RSNO produce *in vivo* both arterial (effect on MAP) and venous (effect on
 462 PAP) dilations. Despite the lack of report on PAP data, this can be assumed even for
 463 SNOPCs, with regards to the raw blood pressure recordings provided by Heikal *et al.* [14].
 464 This is also the case for SNP but not for ISDN, which only produces a decrease in PAP,
 465 reflecting venodilation.

466 Second, regarding the arterial effect, RSNO seem less efficient than SNP, as they
 467 require a 20 to 40-fold higher *NO-load to produce similar hypotension. However, they appear
 468 safer, with a larger margin of safety, as they do not release cyanate leading to toxicity and
 469 death as observed at the end of this study (injection of SNP). The protocol used by Heikal *et*
 470 *al.* did not allow us to compare the arterial effect of SNOPCs to that of the drugs used in the
 471 present report as 1) the different routes of administration used (subcutaneous *vs.* intravenous)
 472 obviously imply a different dose range and 2) hemodynamics were not recorded in the same
 473 conditions (awake rats *vs.* anesthetized mice).

474 Third, regarding the venous effect (the main effect of ISDN and other organic nitrates
475 explaining their use in angina pectoris, for instance, as venodilation decreases cardiac
476 preload), RSNO seem more efficient than ISDN as they produce, for a much lower $\dot{\text{NO}}$ -load,
477 a comparable effect (-15 mmHg in PAP) which lasts longer. For example, $\text{BUC}(\text{NO})_2$ induces
478 the same effect duration on PAP (37 min) than ISDN but with a 6-fold lower $\dot{\text{NO}}$ -load.

479 Finally, more than the total amount of administered $\dot{\text{NO}}$, the nature of the carrier and
480 the number of SNO moieties seem to be major determinants of the biological activities of
481 RSNO. At high doses, $\text{BUC}(\text{NO})_2$ produced the most pronounced decrease in MAP (-62
482 mmHg), an effect that tend to be superior to that of the SNAP+NACNO mixture exhibiting
483 the same $\dot{\text{NO}}$ -load (Figure 6 and Tables 2 and 4). This differential effect at high doses seems
484 to be rather the consequence of a plateau effect reached at the medium dose for
485 SNAP+NACNO, as the highest dose did not produce any further reduction in MAP. This does
486 not seem to be the case for $\text{BUC}(\text{NO})_2$ as the highest dose induced a twofold higher impact on
487 MAP variation compared with the medium dose. This is probably related to the faster
488 metabolism of $\text{BUC}(\text{NO})_2$ as suggested by our *in silico* findings and confirmed by our new
489 data obtained in plasma. As the release of the first $\dot{\text{NO}}$ moiety facilitates the release of the
490 second one (see below), this likely contributes to reach higher levels of $\dot{\text{NO}}$ than with the
491 SNAP+NACNO mixture. Similar results were obtained by Heikal *et al.* when they
492 administered SNOPCs and GSNO *in vivo* at equal molar concentrations of SNO. The SNOPC
493 carrying 6 SNO moieties induced a more pronounced decrease in blood pressure than GSNO
494 or the SNOPC carrying 2 SNO [14]. Taken together, these data suggest that the intrinsic
495 molecular characteristics of the SNO-carrier are a key determinant of the RSNO biological
496 activity. In the present work, we have studied the $\dot{\text{NO}}$ dissociation mechanism in $\text{BUC}(\text{NO})_2$
497 and compared the results to those previously obtained for SNAP and NACNO [20]. As
498 discussed before, the homolytic dissociation in SNAP and NACNO can be assumed to be a
499 barrierless process. The calculated reaction free energies for $\dot{\text{NO}}$ dissociation in SNAP and
500 NACNO were 12.8 and 17.8 kcal.mol⁻¹, respectively [20]. For $\text{BUC}(\text{NO})_2$, all dissociation
501 processes lie within the range of 16-17 kcal.mol⁻¹, which suggests that dissociation in
502 $\text{BUC}(\text{NO})_2$ is significantly less favorable than in SNAP and slightly more favorable than in
503 NACNO. However, $\text{BUC}(\text{NO})_2$ induced the shortest *in vivo* observed effects (Table 4).

504 Several explanations could contribute to this discrepancy. First, given the adopted
505 assumptions in our calculations, these kinetic constant values are only approximations to the
506 real experimental values. Moreover, the *in silico* theoretical results cannot augur for a
507 potential faster degradation rate for $\text{BUC}(\text{NO})_2$ than for NACNO and SNAP *in vivo*. Indeed,

508 we previously showed *in vitro* that the denitrosation pathway [12; 31] of BUC(NO)₂ depends
509 on the protein disulfide isomerase (PDI) activity, which is not the case for either NACNO or
510 SNAP [11]. While this remains to be evaluated *in vivo*, this could explain why BUC(NO)₂ has
511 a shorter effect compared to mononitrosothiols and the mixture. In their studies, Heikal *et al.*
512 also tried to explain the differences of [•]NO release from RSNO studying the effect of various
513 enzymes [12]. While PDI has an effect on both GSNO and SNOPCs, γ -glutamyl
514 transpeptidase only had an effect on GSNO. Taken together, these results highlight the
515 importance of enzyme-dependent metabolism in the observed difference of RSNO action.

516 Finally, the faster [•]NO release from BUC(NO)₂ could also rely on specific physico-
517 chemical properties such as the molecular electronic structure of BUC(NO)₂. After the release
518 of the first [•]NO moiety (possibly related to enzymatic processes, as suggested above), the
519 resulting sulfur free radical reacts with the remaining SNO group leading to the immediate
520 release of the second [•]NO moiety and formation of an intramolecular disulfide bond (Figure
521 1). This was confirmed by the LC-MS/MS analysis of the degradation products of BUC(NO)₂
522 under two operating conditions (heating and exposure to an oxidizing agent *i.e.* H₂O₂)
523 showing the presence of a degradation product including an intramolecular disulfide bond
524 (Figure 2). A similar hypothesis has been proposed for SNOPCs, as they are prone to a more
525 rapid physicochemical degradation *in vitro* than GSNO, which correlates with the formation
526 of intramolecular disulfide bonds, assessed by mass spectrometry [32]. This fast release of the
527 first [•]NO moiety followed by the formation of an intramolecular disulfide bridge can
528 contribute to the faster metabolism of BUC(NO)₂ observed *in vitro* in plasma and thus to the
529 its shorter effect compared to NACNO and SNAP. The more lipophilic nature of BUC(NO)₂
530 compared to SNAP and NACNO (Table 3, [11]) could also contribute to the faster [•]NO
531 release. When administered subcutaneously, the lipophilic properties of BUC(NO)₂ may
532 accelerate its flow through cellular membranes within blood vessels and thus lead to a faster
533 systemic effect.

534 In the field of RSNO and their clinical use, the most important challenge actually is to
535 control kinetics and amounts of [•]NO to be released, especially during pathologies where
536 oxidative stress may lead to nitrosative derivation of [•]NO when released from RSNO [33]. In
537 this context, the capacity of BUC(NO)₂ to quickly release a great quantity of [•]NO may be
538 considered as a disadvantage. However, when compared to other commercially available fast
539 [•]NO donors such as SNP, BUC(NO)₂ would certainly not induce side effects, as bucillamine,
540 when used as an anti-inflammatory and antioxidant agent, does not produce serious adverse
541 events [16]. Furthermore, as lipophilic molecules are easier to encapsulate [34], formulation

542 of BUC(NO)₂ would be a good strategy to increase duration of its effects in pathologies that
543 requires a slow and sustained release of [•]NO (*e.g.* post-stroke, [17]).

544 As a conclusion, the hypothesis that increasing [•]NO payload on polythiols would
545 increase the efficiency of corresponding RSNO seems to depend on the nature of the thiolated
546 molecule carrying [•]NO. Rather than increasing the number of [•]NO, attention must be payed to
547 the choice of the molecule carrying [•]NO, as numerous factors are involved in the degradation
548 of RSNO.

549 **ACKNOWLEDGMENTS**

550 **FUNDING SOURCES**

551 This work was supported by the French Ministry of Research and Education (Paris, France).

552 **DISCLOSURES**

553 None

554 **REFERENCES**

- 555 [1] S. Moncada, E.A. Higgs, Endogenous nitric oxide: physiology, pathology and clinical
556 relevance, *Eur. J. Clin. Invest.* 21 (1991) 361-74.
- 557 [2] J.A. Bauer, H.L. Fung, Differential hemodynamic effects and tolerance properties of
558 nitroglycerin and an S-nitrosothiol in experimental heart failure, *J. Pharmacol. Exp. Ther.* 256
559 (1991) 249-54.
- 560 [3] J.D. Parker, T. Gori, Tolerance to the organic nitrates: new ideas, new mechanisms,
561 continued mystery, *Circulation* 104 (2001) 2263-5.
- 562 [4] U. Förstermann, T. Münzel, Endothelial nitric oxide synthase in vascular disease: from
563 marvel to menace, *Circulation* 113 (2006) 1708-14.
- 564 [5] C. Gaucher, A. Boudier, F. Dahboul, M. Parent, P. Leroy, S-nitrosation/denitrosation in
565 cardiovascular pathologies: facts and concepts for the rational design of S-nitrosothiols, *Curr.*
566 *Pharm. Des.* 19 (2013) 458-72.
- 567 [6] C. Mancuso, A. Bonsignore, E. Di Stasio, A. Mordente, R. Motterlini, Bilirubin and S-
568 nitrosothiols interaction: evidence for a possible role of bilirubin as a scavenger of nitric
569 oxide, *Biochem. Pharmacol.* 66 (2003) 2355-63.
- 570 [7] J.L. Alencar, I. Lobysheva, K. Chalupsky, M. Geffard, F. Nepveu, J.C. Stoclet, B. Muller,
571 S-nitrosating nitric oxide donors induce long-lasting inhibition of contraction in isolated
572 arteries, *J. Pharmacol. Exp. Ther.* 307 (2003) 152-9.
- 573 [8] B. Furlong, A.H. Henderson, M.J. Lewis, J.A. Smith, Endothelium-derived relaxing factor
574 inhibits in vitro platelet aggregation, *Br. J. Pharmacol.* 90 (1987) 687-92.
- 575 [9] H. Al-Sa'doni, A. Ferro, S-nitrosothiols as nitric oxide-donors: chemistry, biology and
576 possible future therapeutic applications, *Curr. Med. Chem.* 11 (2004) 2679-90.
- 577 [10] W. Wu, C. Perrin-Sarrado, H. Ming, I. Lartaud, P. Maincent, X.M. Hu, A. Sapin-Minet,
578 C. Gaucher, Polymer nanocomposites enhance S-nitrosoglutathione intestinal absorption and
579 promote the formation of releasable nitric oxide stores in rat aorta, *Nanomed. Nanotechnol.*
580 *Biol. Med.* 12 (2016) 1795-1803.
- 581 [11] F. Dahboul, C. Perrin-Sarrado, A. Boudier, I. Lartaud, R. Schneider, P. Leroy, S,S'-
582 dinitrosobucillamine, a new nitric oxide donor, induces a better vasorelaxation than other S-
583 nitrosothiols, *Eur. J. Pharmacol.* 730 (2014) 171-9.
- 584 [12] L. Heikal, P.I. Aaronson, A. Ferro, M. Nandi, G.P. Martin, L.A. Dailey, S-
585 nitrosophytochelatin: investigation of the bioactivity of an oligopeptide nitric oxide delivery
586 system, *Biomacromolecules* 12 (2011) 2103-13.
- 587 [13] I.L. Megson, I.R. Greig, A.R. Butler, G.A. Gray, D.J. Webb, Therapeutic potential of S-
588 nitrosothiols as nitric oxide donor drugs, *Scott. Med. J.* 42 (1997) 88-9.
- 589 [14] L. Heikal, A. Starr, G.P. Martin, M. Nandi, L.A. Dailey, In vivo pharmacological activity
590 and biodistribution of S-nitrosophytochelatin after intravenous and intranasal administration
591 in mice, *Nitric Oxide* 59 (2016) 1-9.
- 592 [15] L.D. Horwitz, Bucillamine: a potent thiol donor with multiple clinical applications,
593 *Cardiovasc. Drug Rev.* 21 (2003) 77-90.
- 594 [16] N. Sekiguchi, H. Kameda, K. Amano, T. Takeuchi, Efficacy and safety of bucillamine, a
595 D-penicillamine analogue, in patients with active rheumatoid arthritis, *Mod. Rheumatol.* 16
596 (2006) 85-91.

- 597 [17] M. Parent, A. Boudier, F. Dupuis, C. Nouvel, A. Sapin, I. Lartaud, J.L. Six, P. Leroy, P.
598 Maincent, Are in situ formulations the keys for the therapeutic future of S-nitrosothiols?, Eur.
599 J. Pharm. Biopharm. 85 (2013) 640-649.
- 600 [18] M. Parent, A. Boudier, J. Perrin, C. Vigneron, P. Maincent, N. Violle, J.F. Bisson, I.
601 Lartaud, F. Dupuis, In Situ Microparticles Loaded with S-Nitrosoglutathione Protect from
602 Stroke, PLoS One 10 (2015) e0144659.
- 603 [19] M. Parent, F. Dahboul, R. Schneider, I. Clarot, P. Maincent, P. Leroy, A. Boudier, A
604 complete physicochemical identity card of S-nitrosoglutathione, Curr. Pharm. Anal. 9 (2013)
605 31-42.
- 606 [20] B. Meyer, A. Genoni, A. Boudier, P. Leroy, M.F. Ruiz-Lopez, Structure and Stability
607 Studies of Pharmacologically Relevant S-Nitrosothiols: A Theoretical Approach, J. Phys.
608 Chem. A 120 (2016) 4191-200.
- 609 [21] J.P. Perdew, Y. Wang, Accurate and simple analytic representation of the electron-gas
610 correlation energy, Phys Rev B Condens Matter 45 (1992) 13244-13249.
- 611 [22] E. Cancès, B. Mennucci, J. Tomasi, A new integral equation formalism for the
612 polarizable continuum model: Theoretical background and applications to isotropic and
613 anisotropic dielectrics., J. Chem. Phys. 107 (1997) 3032-3041.
- 614 [23] M.J. Frisch, G.W. Trucks, H.B. Schlegel, G.E. Scuseria, M.A. Robb, J.R. Cheeseman, G.
615 Scalmani, V. Barone, B. Mennucci, G.A. Petersson, H. Nakatsuji, M. Caricato, X. Li, H.P.
616 Hratchian, A.F. Izmaylov, J. Bloino, G. Zheng, J.L. Sonnenberg, M. Hada, M. Ehara, K.
617 Toyota, R. Fukuda, J. Hasegawa, M. Ishida, T. Nakajima, Y. Honda, O. Kitao, H. Nakai, T.
618 Vreven, J.A. Montgomery Jr., J.E. Peralta, F. Ogliaro, M.J. Bearpark, J. Heyd, E.N. Brothers,
619 K.N. Kudin, V.N. Staroverov, R. Kobayashi, J. Normand, K. Raghavachari, A.P. Rendell, J.C.
620 Burant, S.S. Iyengar, J. Tomasi, M. Cossi, N. Rega, N.J. Millam, M. Klene, J.E. Knox, J.B.
621 Cross, V. Bakken, C. Adamo, J. Jaramillo, R. Gomperts, R.E. Stratmann, O. Yazyev, A.J.
622 Austin, R. Cammi, C. Pomelli, J.W. Ochterski, R.L. Martin, K. Morokuma, V.G. Zakrzewski,
623 G.A. Voth, P. Salvador, J.J. Dannenberg, S. Dapprich, A.D. Daniels, Ö. Farkas, J.B.
624 Foresman, J.V. Ortiz, J. Cioslowski, D.J. Fox, Gaussian 09, Gaussian, Inc., Wallingford, CT,
625 USA, 2009.
- 626 [24] P. Pikul, M. Jamrogiewicz, J. Nowakowska, W. Hewelt-Belka, K. Ciura, Forced
627 Degradation Studies of Ivabradine and In Silico Toxicology Predictions for Its New
628 Designated Impurities, Front. Pharmacol. 7 (2016) 117.
- 629 [25] J. Sun, X. Zhang, M. Broderick, H. Fein, Measurement of Nitric Oxide Production in
630 Biological Systems by Using Griess Reaction Assay, Sensors 3 (2003) 276-284.
- 631 [26] N. Sogo, C. Campanella, D.J. Webb, I.L. Megson, S-nitrosothiols cause prolonged, nitric
632 oxide-mediated relaxation in human saphenous vein and internal mammary artery: therapeutic
633 potential in bypass surgery, Br. J. Pharmacol. 131 (2000) 1236-44.
- 634 [27] N. Niederhoffer, V. Marque, I. Lartaud-Idjouadiene, C. Duviol, R. Peslin, J. Atkinson,
635 Vasodilators, aortic elasticity, and ventricular end-systolic stress in nonanesthetized
636 unrestrained rats, Hypertension 30 (1997) 1169-74.
- 637 [28] T. Rassaf, L.W. Poll, P. Brouzos, T. Lauer, M. Totzeck, P. Kleinbongard, P. Gharini, K.
638 Andersen, R. Schulz, G. Heusch, U. Modder, M. Kelm, Positive effects of nitric oxide on left
639 ventricular function in humans, Eur. Heart J. 27 (2006) 1699-705.

- 640 [29] D. Giustarini, A. Milzani, I. Dalle-Donne, R. Rossi, Detection of S-nitrosothiols in
641 biological fluids: a comparison among the most widely applied methodologies, *J. Chromatogr.*
642 *B* 851 (2007) 124-139.
- 643 [30] E. Bramanti, V. Angeli, Z. Mester, A. Pompella, A. Paolicchi, A. D'Ulivo, Determination
644 of S-nitrosoglutathione in plasma: comparison of two methods, *Talanta* 81 (2010) 1295-9.
- 645 [31] R. Xiao, J. Lundström-Ljung, A. Holmgren, H.F. Gilbert, Catalysis of thiol/disulfide
646 exchange. Glutaredoxin 1 and protein-disulfide isomerase use different mechanisms to
647 enhance oxidase and reductase activities, *J. Biol. Chem.* 280 (2005) 21099-106.
- 648 [32] L. Heikal, G.P. Martin, L.A. Dailey, Characterisation of the decomposition behaviour of
649 S-nitrosoglutathione and a new class of analogues: S-Nitrosophytochelatin, *Nitric Oxide* 20
650 (2009) 157-65.
- 651 [33] Y. Liu, C. Xia, R. Wang, J. Zhang, T. Yin, Y. Ma, L. Tao, The opposite effects of nitric
652 oxide donor, S-nitrosoglutathione, on myocardial ischemia/reperfusion injury in diabetic and
653 non-diabetic mice, *Clin. Exp. Pharmacol. Physiol.* (2017).
- 654 [34] M. Parent, C. Nouvel, M. Koerber, A. Sapin, P. Maincent, A. Boudier, PLGA in situ
655 implants formed by phase inversion: critical physicochemical parameters to modulate drug
656 release, *J. Control. Release* 172 (2013) 292-304.
- 657